suppressed rainfall rate (maximum vertical velocity) around 17 LST (Figs. 8.21a-b). These results are in agreement with previous studies (e. g., Emanuel and Raymond 1994). The diurnal variation of maximum heat flux is more sinusoidal (Fig. 8.21c). The heat flux exhibits maximum around 20 LST and minimum around 09 LST. This variation is caused by the difference between sea and air temperature which is directly proportional to the sensible heat flux across the air-sea interface and by the variation in wind speeds which determines the latent heat flux.

During the ENSO event, no significant diurnal variation is found for the above variables (Figs. 8.22a-c). Significant rainfall starts after 34 hour of integration corresponding to significant minimum vertical velocity. In general, high surface heat fluxes with a maximum of 525 Wm^{-2} are simulated over the Indian Ocean.

8.1 Indonesia

8.2.1 Streamlines and Wind Speeds

Figures 8.23a-d and 8.24a-d display the analyzed and day-1 simulated streamlines and wind speeds for 00 UTC 30 January 1997 obtained from the NRL/NCSU model and the PSU-NCAR MM5, respectively. The onset of the monsoon can be clearly seen in Fig. 8.23a, which shows the organization and strengthening of the low-level westerlies over and to the north of northern Australia. In general, both models are able to simulate the mean flows such as westerly wind convergence over the southeastern Indian Ocean and low-level pressure over northern Australia quite reasonably. In contrast, in all grid resolutions the NRL/NCSU model does not produce the low-level pressure system over Kalimantan realistically (Figs. 8.23a-d). Also, the wind speeds of the westerly

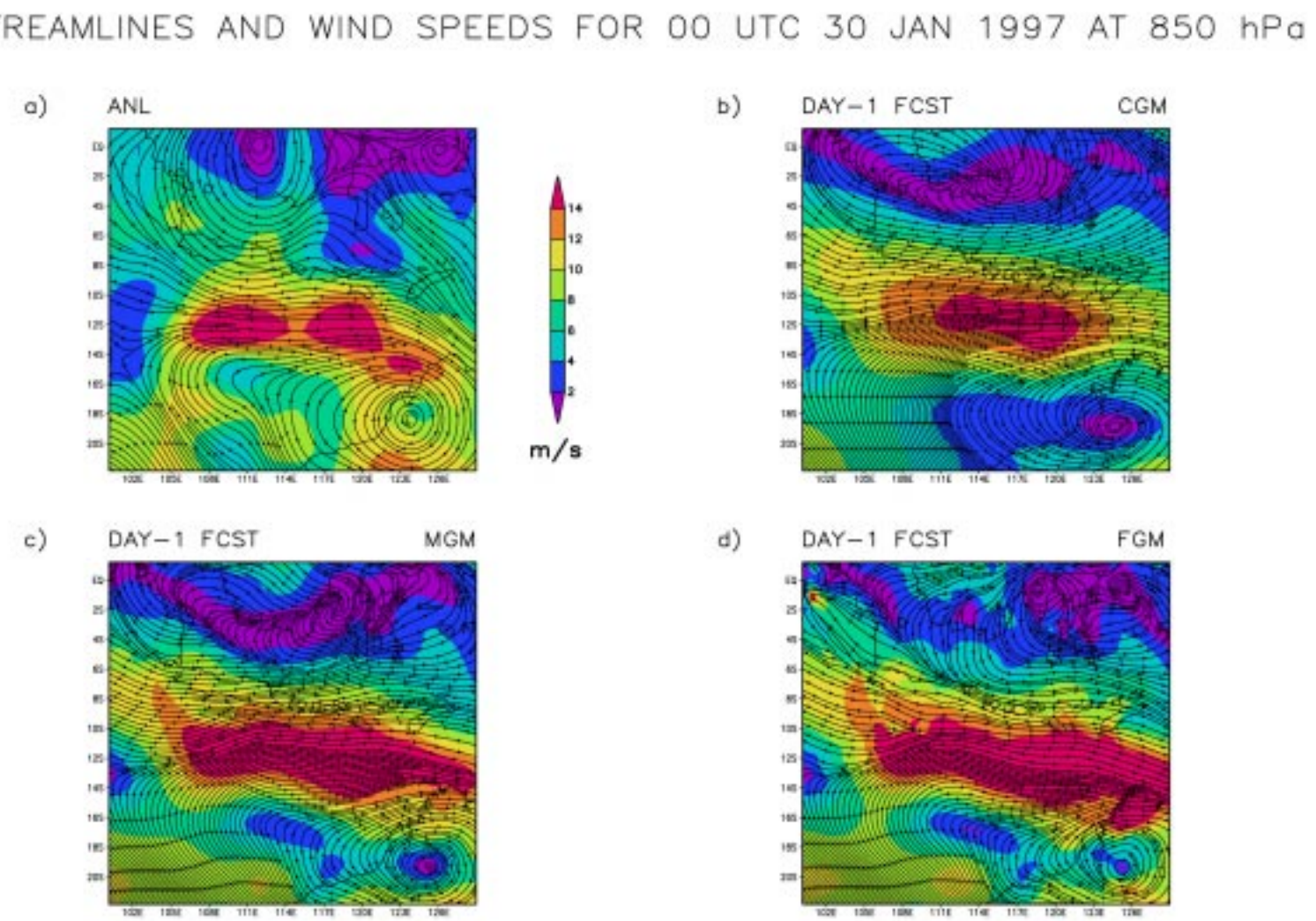

Figure 8.23. a) The analyzed and day-1 simulated streamlines and wind speeds for 00 UTC 30 January 1997 at 850 hPa in b) CGM, c) MGM, and d) FGM grid resolutions for the Indonesia case from the NRL/NCSU model.

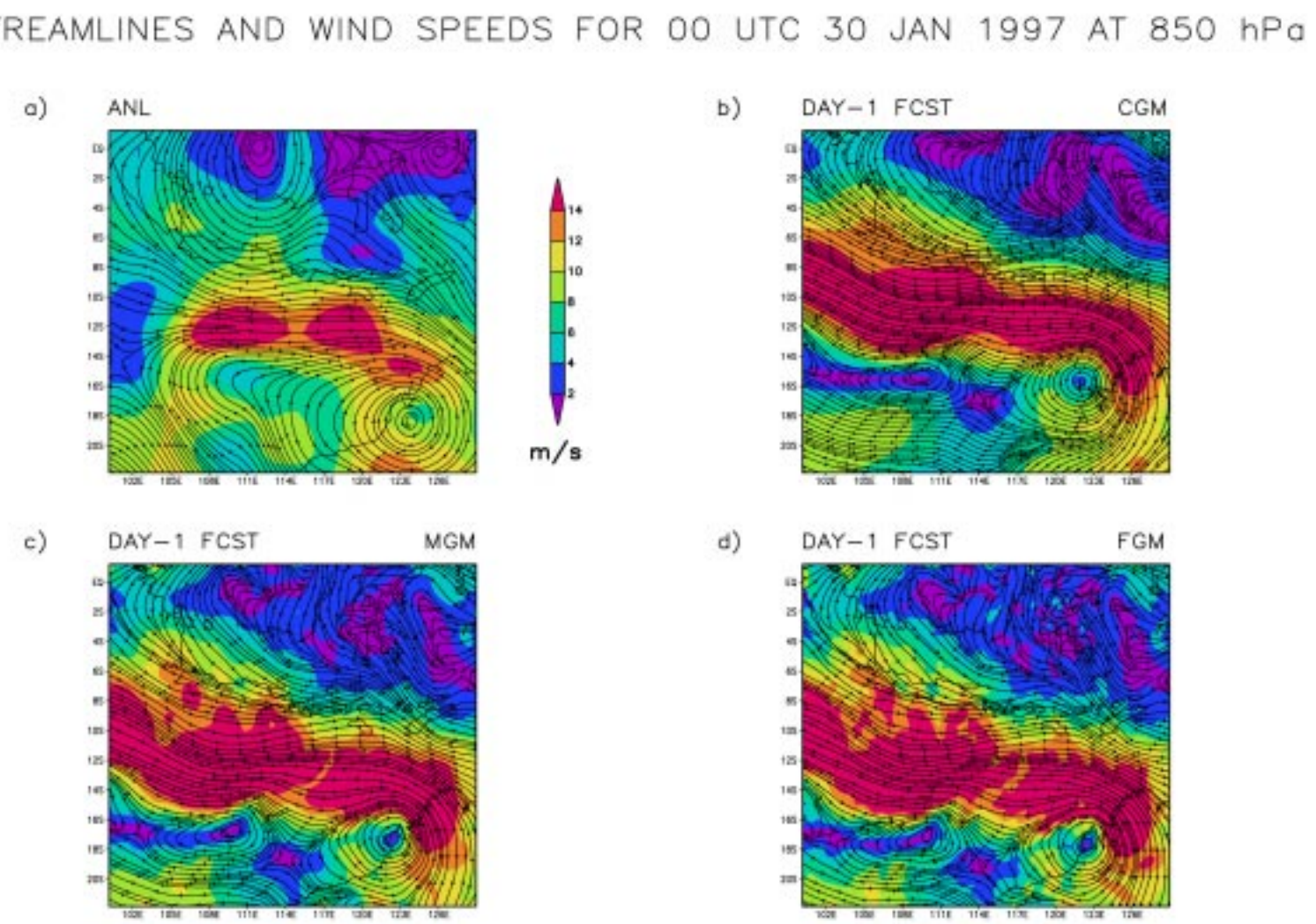

Figure 8.24. As in Fig. 8.23, except from the PSU-NCAR MM5.

convergence are slightly overestimated, while those in the equator are underestimated. Similarly, the PSU-NCAR MM5 is not able to simulate the low-level pressure system over Kalimantan accurately (Figs. 8.24a-d). However, it simulates cyclonic eddies over the southern Indian Ocean between 14°S and 18°S. The wind speeds of the westerly convergence over the southeastern Indian Ocean are also overestimated. The forecast skills in Table 8.2 shows that the NRL/NCSU model result in smaller BIAS and RMSE values for both U and V components than the PSU-NCAR MM5. It also has higher CORR values as compared to the PSU-NCAR MM5.

At 00 UTC 31 January 1997, both the NRL/NCSU model and the PSU-NCAR MM5 are able to retain the westerly convergence winds over the southeastern Indian Ocean (Figs. 8.25a-d and 8.26a-d). The corresponding wind speeds are more accurately predicted by the PSU-NCAR MM5. On the other hand, the NRL/NCSU model simulates the low-pressure system over northern Australia and the northeasterly cross-equatorial flows reasonably well. The PSU-NCAR MM5 has lower BIAS and RMSE values for U component, but higher for V component compared to the NRL/NCSU model. Nevertheless, the NRL/NCSU model has overall higher CORR values than the PSU-NCAR MM5.

Figures 8.27a-d and 8.28a-d show the analyzed and day-1 simulated streamlines and wind speeds for 00 UTC 30 January 1998 obtained from the NRL/NCSU model and the PSU-NCAR MM5, respectively. In general, both models do produce the low-pressure system in northern Australia and the southern Indian Ocean at (19°S; 107°E), the westerly winds over the southeastern Indian Ocean, and the cross-equatorial flows over the Java sea quite reasonably. Nevertheless, the location of the low-pressure system and

Table 8.2. As in Table 8.1, except for the Indonesia case.

Date	Var.	Mean (ms^{-1})			BIAS (ms^{-1})		RMSE (ms^{-1})		CORR	
		ANL	NCSU	MM5	NCSU	MM5	NCSU	MM5	NCSU	MM5
00 UTC 30 Jan 97	U	3.5	5.6	5.8	2.1	2.3	6.6	8.1	0.60	0.41
	V	0.5	0.2	-2.2	-0.4	-2.7	3.7	5.4	0.60	0.38
00 UTC 31 Jan 97	U	2.6	5.4	2.6	2.8	0.1	6.9	6.3	0.45	0.30
	V	-0.9	-1.4	-2.1	-0.5	-1.2	4.0	5.7	0.66	0.17
00 UTC 30 Jan 98	U	2.0	2.5	2.5	0.5	0.5	6.4	6.7	0.41	0.50
	V	-0.6	-2.3	-2.4	-1.7	-1.7	4.1	3.8	0.47	0.62
00 UTC 31 Jan 98	U	2.5	2.9	0.3	0.4	-2.2	7.7	6.7	0.28	0.45
	V	-1.0	-1.8	0.6	-0.8	1.5	5.5	3.5	-0.06	0.74

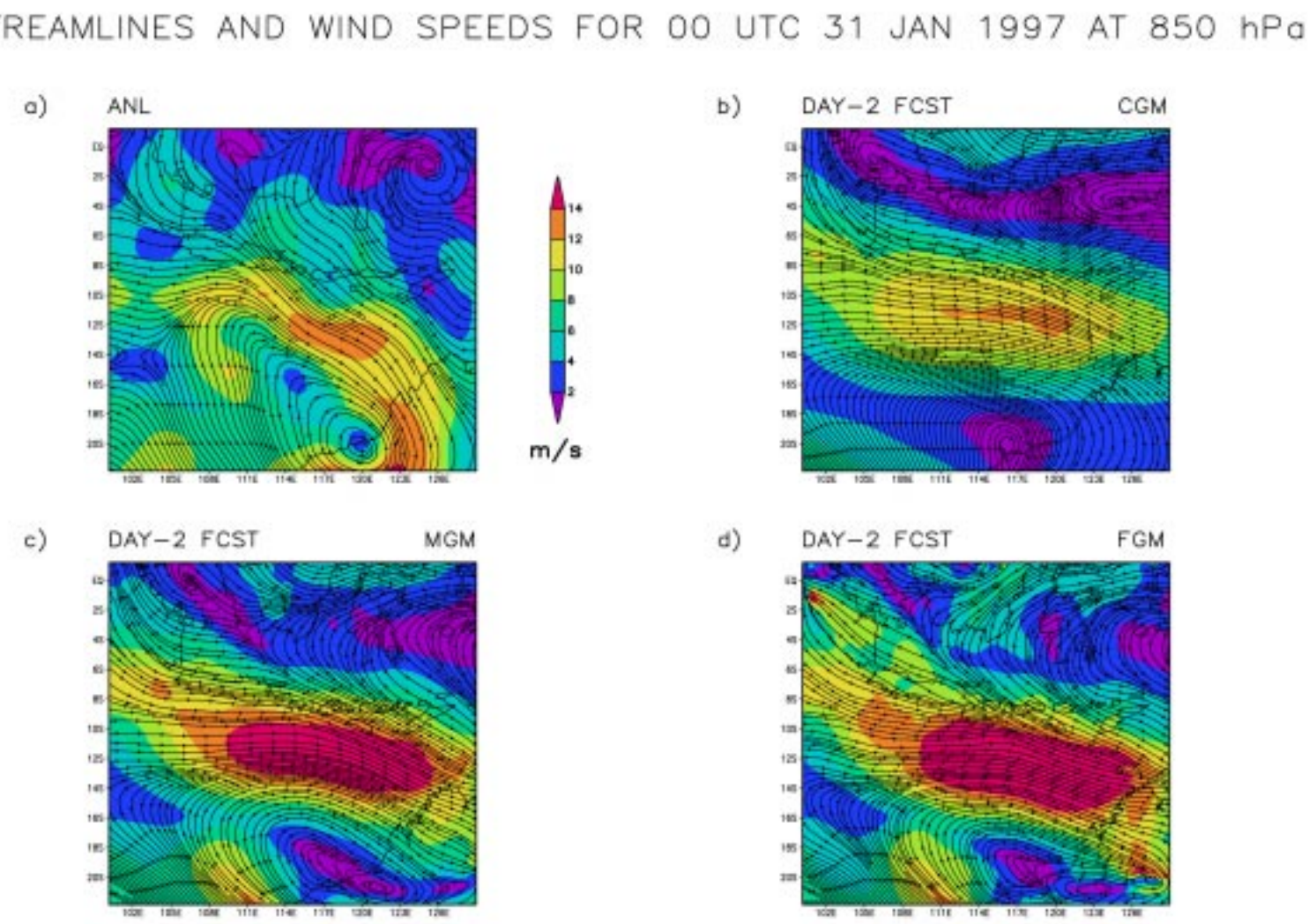

Figure 8.25. a) The analyzed and day-2 simulated streamlines and wind speeds for 00 UTC 31 January 1997 at 850 hPa in b) CGM, c) MGM, and d) FGM grid resolutions for the Indonesia case from the NRL/NCSU model.

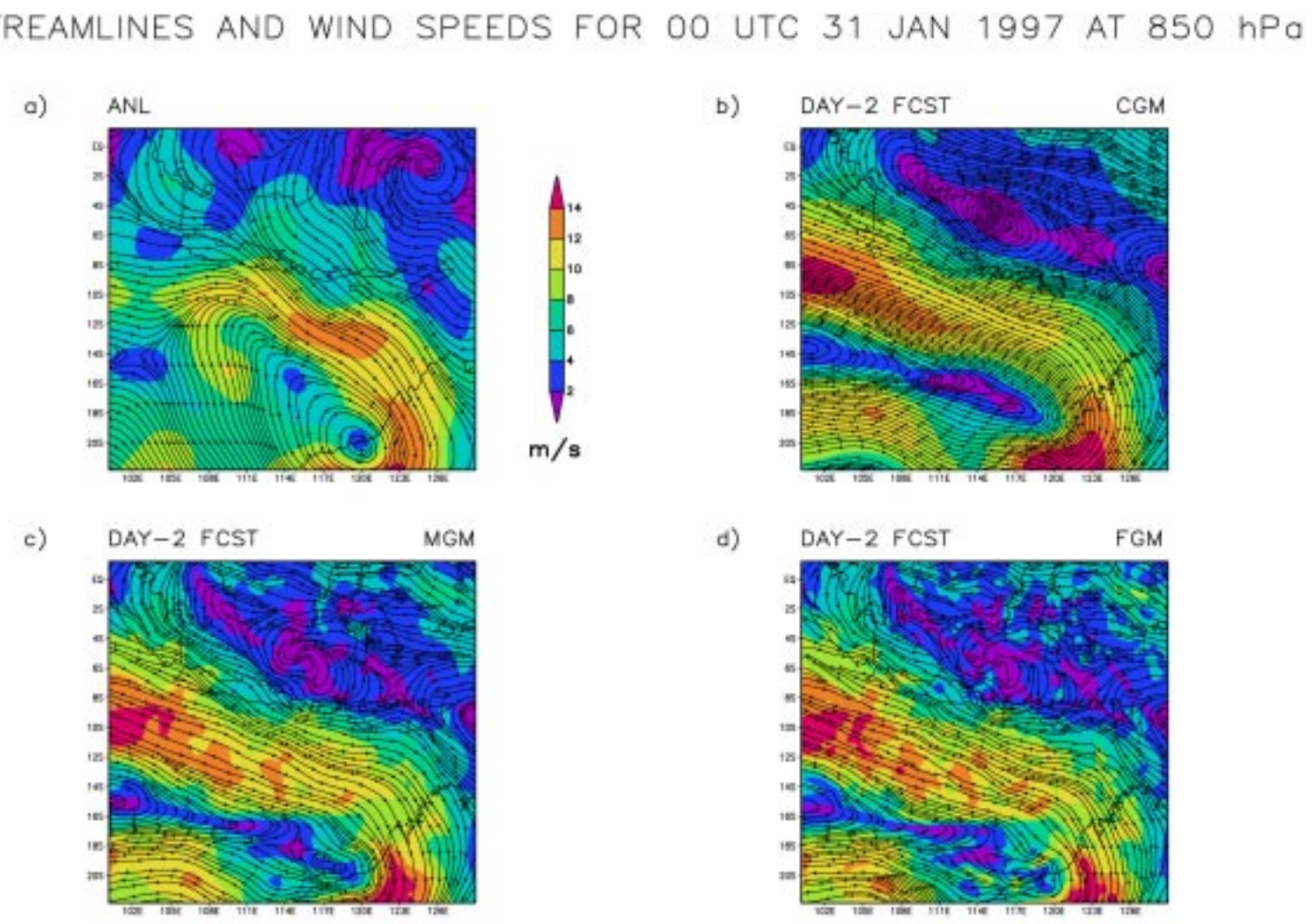

Figure 8.26. As in Fig. 8.25, except from the PSU-NCAR MM5.

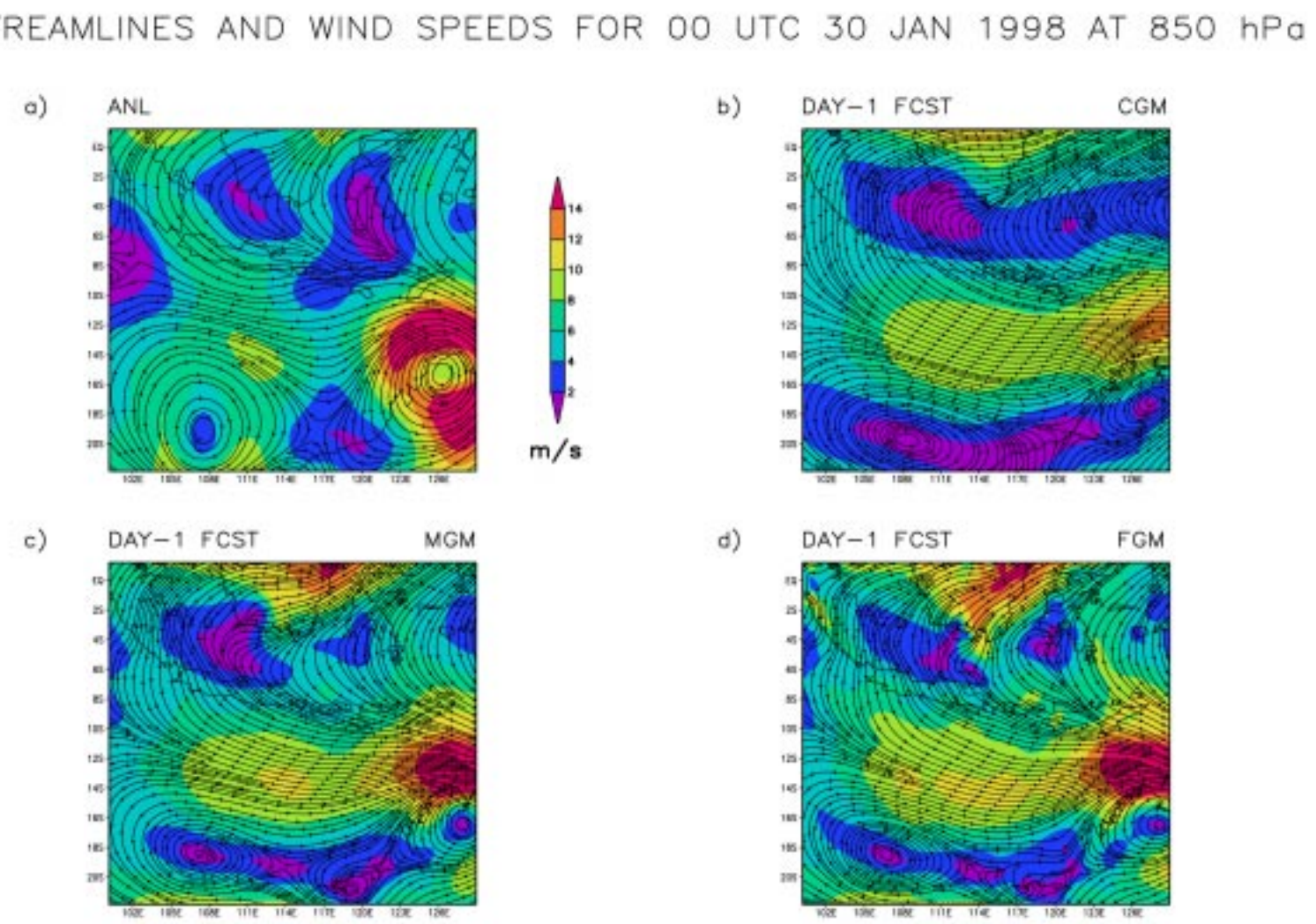

Figure 8.27. a) The analyzed and day-1 simulated streamlines and wind speeds for 00 UTC 30 January 1998 at 850 hPa in b) CGM, c) MGM, and d) FGM grid resolutions for the Indonesia case from the NRL/NCSU model.

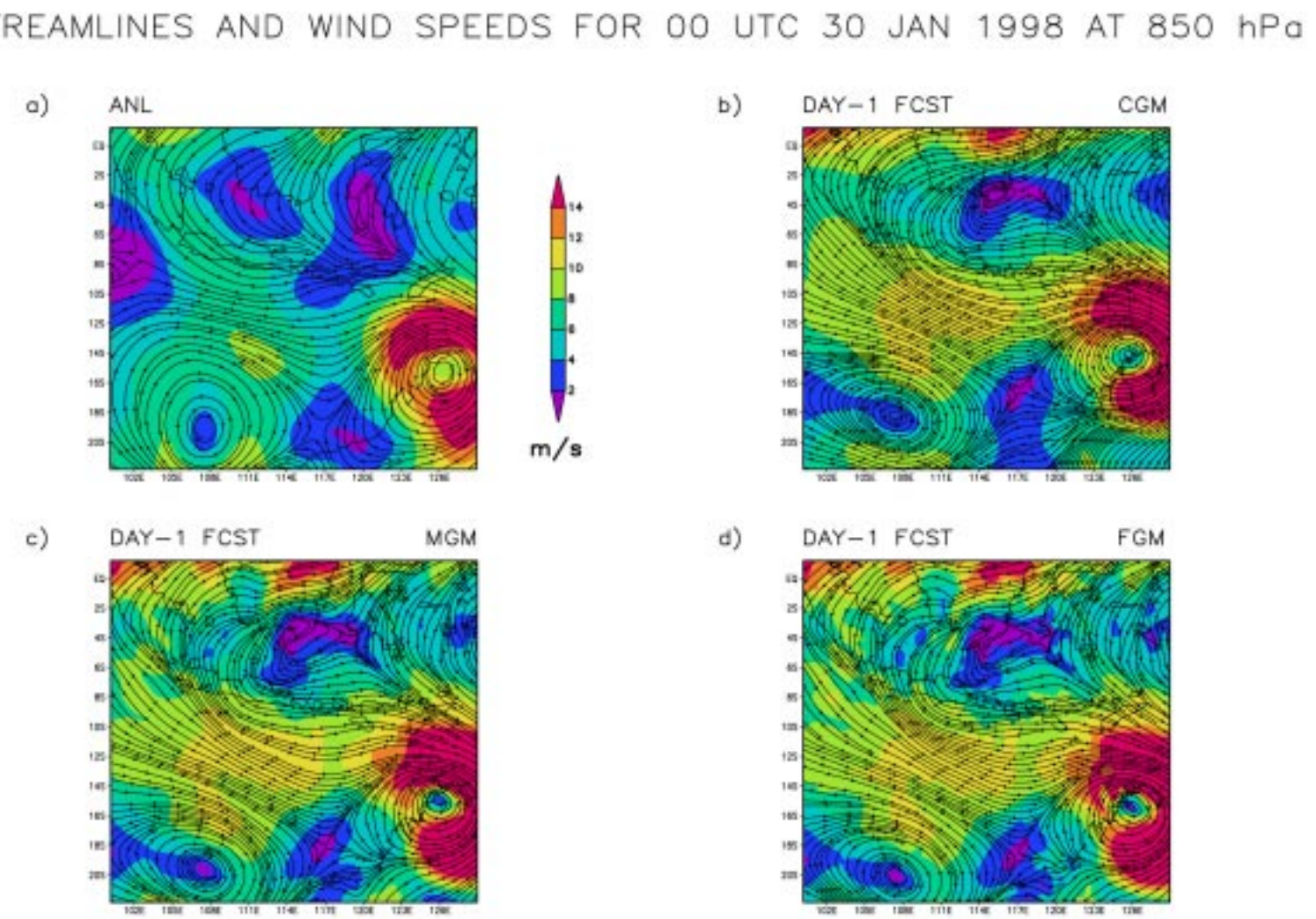

Figure 8.28. As in Fig. 8.27, except from the PSU-NCAR MM5.

its wind speeds over northern Australia are better simulated by the PSU-NCAR MM5 than by the NRL/NCSU model. Although the BIAS and RMSE values for U and V components resulted from both models are almost the same, the PSU-NCAR MM5 has higher values of CORR.

At 00 UTC 31 January 1998, the NRL/NCSU model is unable to maintain and generate the low-pressure system over northern Australia (Figs. 8.29a-d). On the other hand, this system and its corresponding wind speeds are reasonably simulated by the PSU-NCAR MM5 (Figs. 8.30a-d). Both models have difficulties to simulate wind patterns over the land regions. The PSU-NCAR MM5 has the overall CORR values for U and V components higher than that for the NRL/NCSU model.

8.2.2 Rainfall

Figures 8.31a-d and 8.32a-d show the OLR distribution and day-1 simulated accumulated rainfall for 00 UTC 30 January 1997 obtained from the NRL/NCSU model and the PSU-NCAR MM5, respectively. During the 24 hours of integration, the NRL/NCSU model simulates a band of rainfall over the southeastern Indian Ocean with a maximum of 200 mm day^{-1} along (8°S-10°S; 102°E-106°E) and over northern Australia (Figs. 8.31a-d). This band of rainfall is in agreement with low OLR values. Note that the OLR values $\leq$ 200 Wm^{-2} are an indication of convective activity. An improvement in the areal and magnitudes of rainfall is gained as the horizontal resolution is increased. Over the land, rainfall is simulated near the coast and over high topographies. In contrast, the PSU-NCAR MM5 simulates a broad rainfall region along the southern Indian Ocean with a

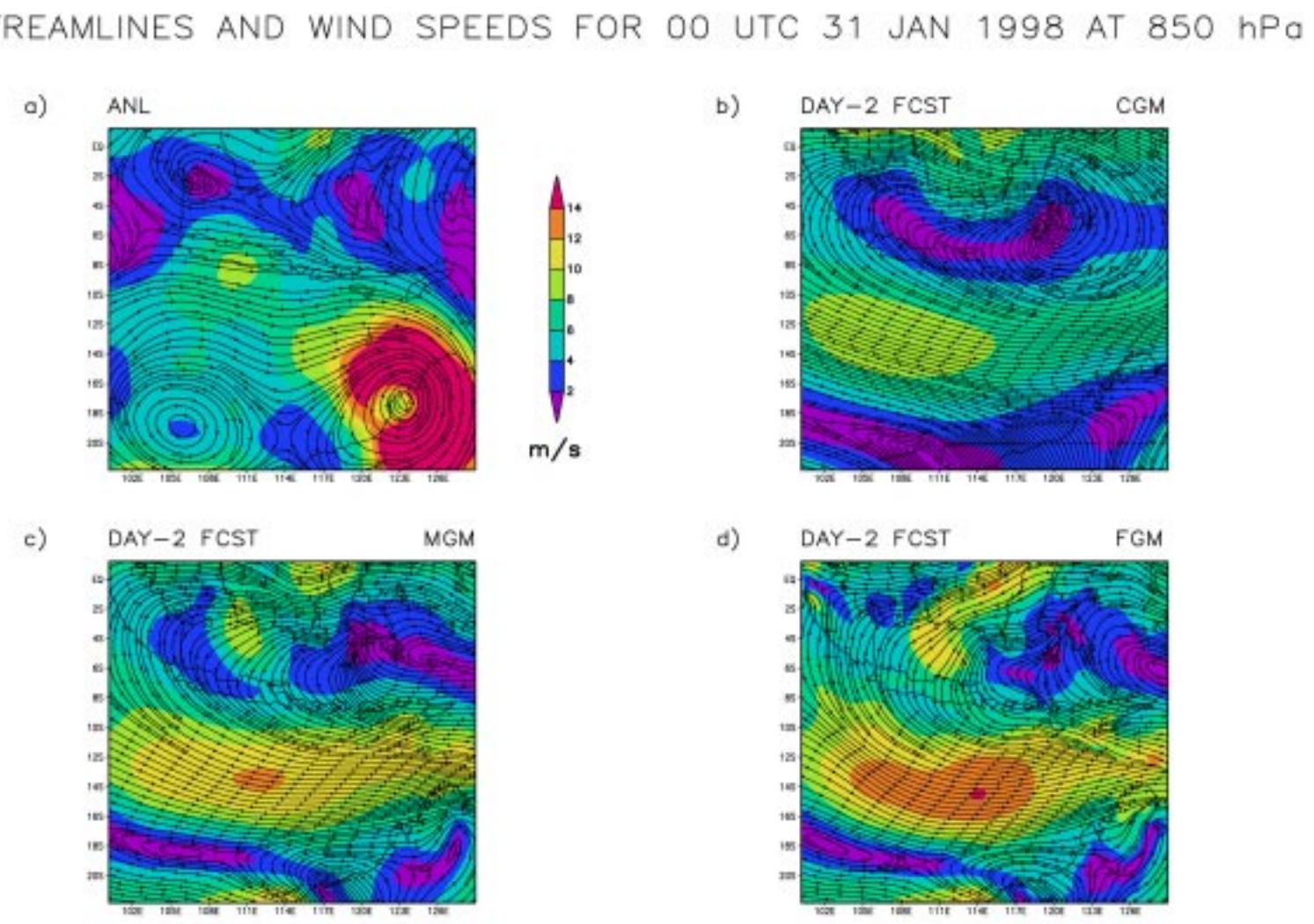

Figure 8.29. a) The analyzed and day-2 simulated streamlines and wind speeds for 00 UTC 31 January 1998 at 850 hPa in b) CGM, c) MGM, and d) FGM grid resolutions for the Indonesia case from the NRL/NCSU model.

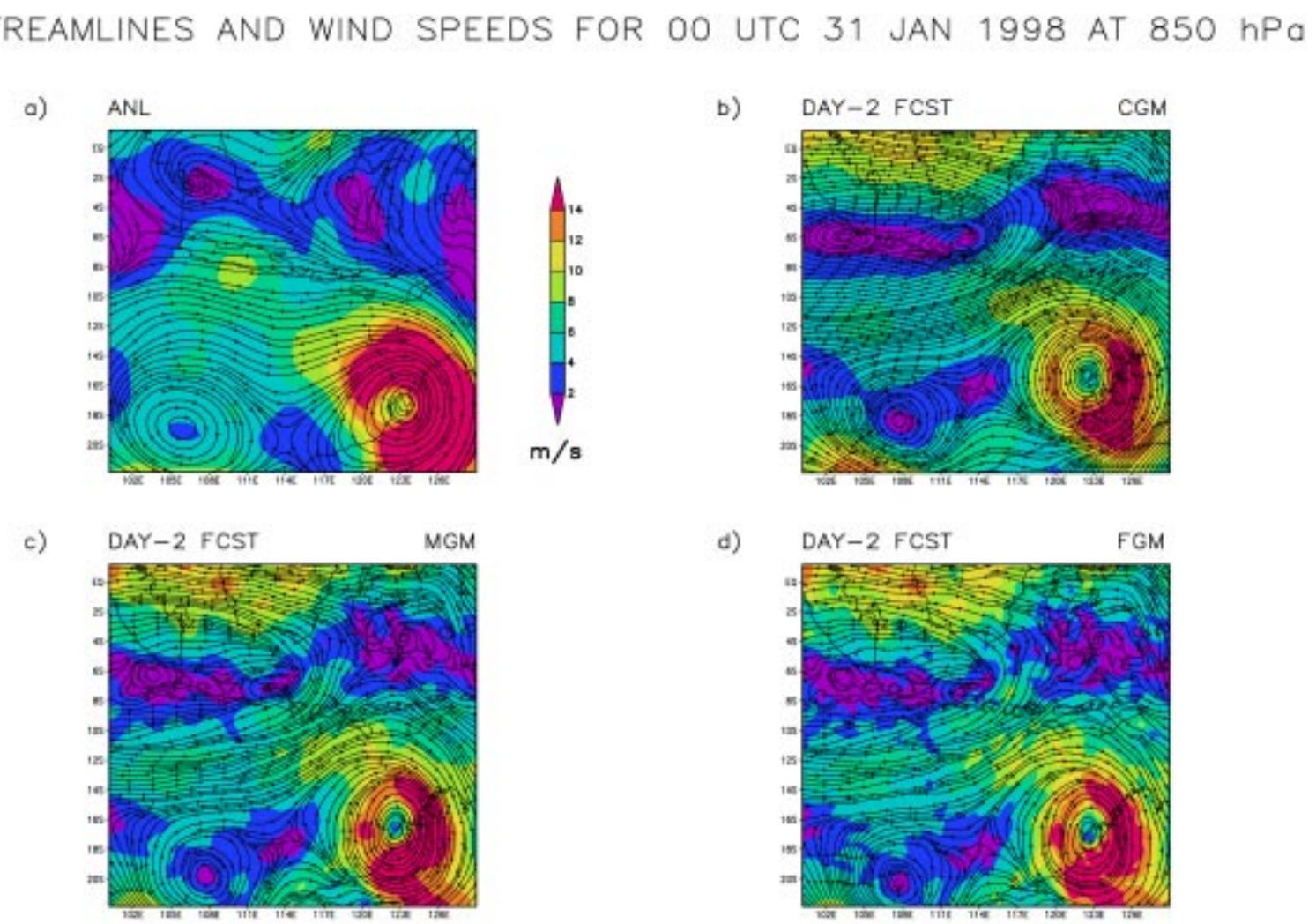

Figure 8.30. As in Fig. 8.29, except from the PSU-NCAR MM5.

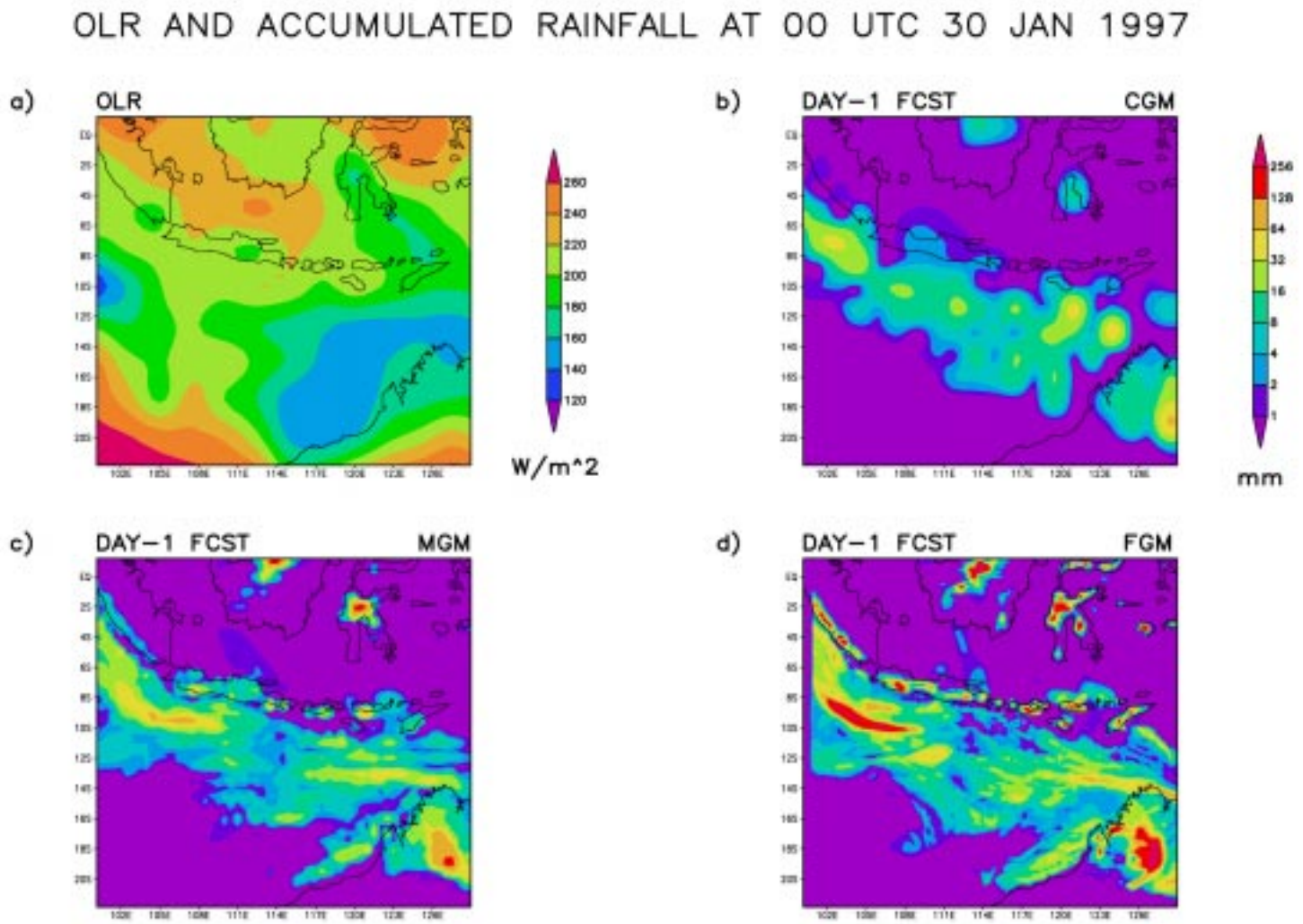

Figure 8.31. a) The OLR distribution and day-1 simulated accumulated rainfall ending at 00 UTC 30 January 1997 in b) CGM, c) MGM, and d) FGM grid resolutions for the Indonesia case from the NRL/NCSU model.

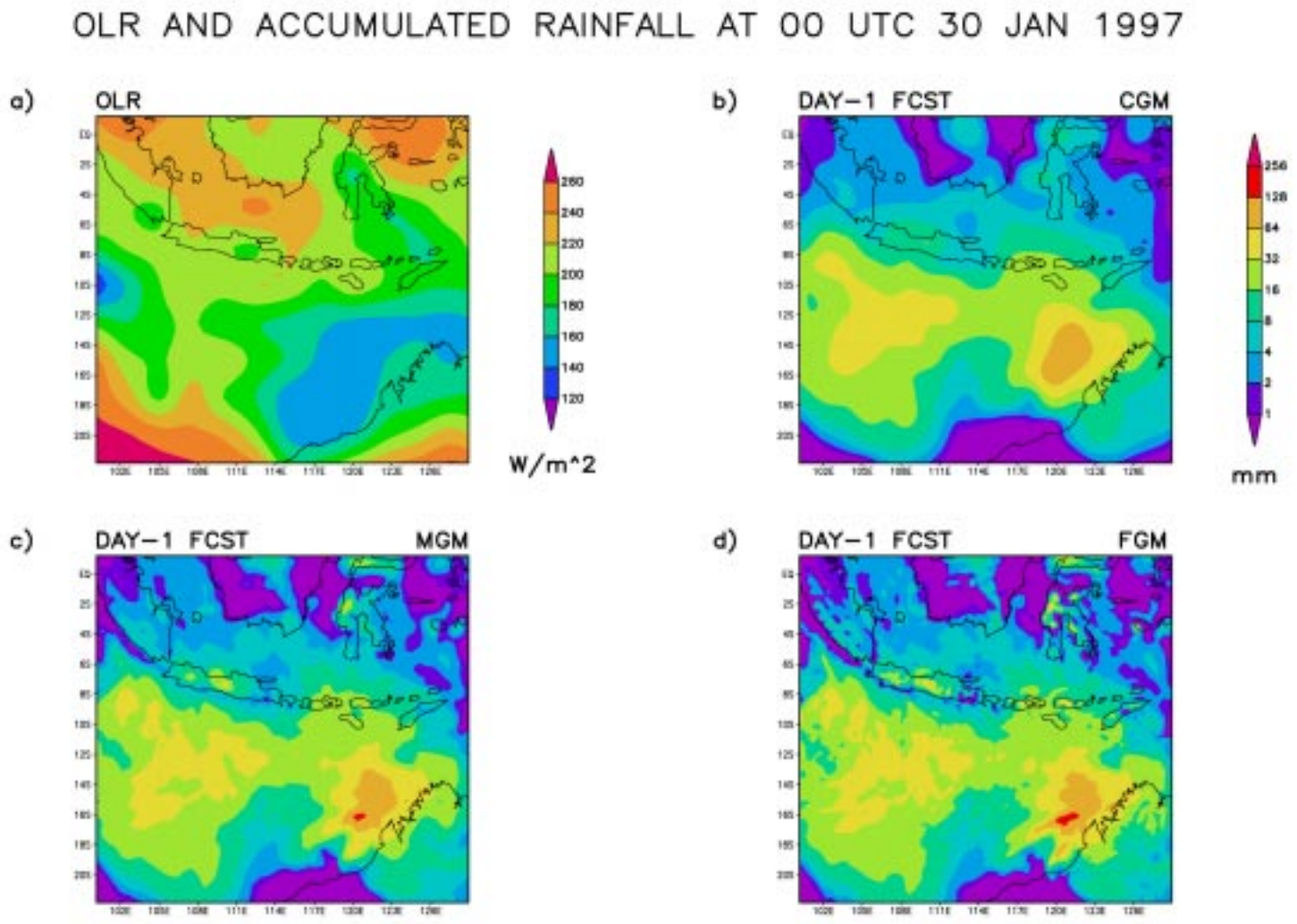

Figure 8.32. As in Fig. 8.31, except from the PSU-NCAR MM5.

maximum of 100 mm day^{-1} (Figs. 8.32a-d). Also, lower rainfall rates in comparison to those from the NRL/NCSU model are found over the lands.

At 00 UTC 31 January 1997, overall rainfall rates are simulated by both the models in correspondence with the OLR data (Figs. 8.33a-d and 8.34a-d). However, the spatial patterns of rain are again different for each model. In the NRL/NCSU model simulation, a band of rainfall no longer exists (Figs 8.33a-d). Significant rainfall occurs mainly over northern Australia with a maximum of 140 mm day^{-1}. A broad area of rainfall covering most of the oceans is still simulated by the PSU-NCAR MM5 (Figs. 8.34a-d). A maximum rainfall of the order of 80 mm day^{-1} occurs over the southeastern Indian Ocean to the west of northern Australia.

Figures 8.35a-d and 8.36a-d show the OLR distribution and day-1 simulated accumulated rainfall for 00 UTC 30 January 1998 obtained from the NRL/NCSU and the PSU-NCAR MM5, respectively. Although convective activity is approximately located over Sumatera, Java, northern Australia, and the surrounding oceans, the NRL/NCSU model captures rainfall activities over all islands in Indonesia and northern Australia region (Figs. 8.35a-d). The PSU-NCAR MM5, on the other hand, simulates rainfall over all the Indonesian-Australian regions (Figs. 8.36a-d). However, rainfall with a maximum of 20 mm day^{-1} is also simulated over the southeastern Indian Ocean (16°S-20°S; 103°E-112°E), which is not consistent with the OLR data.

At 00 UTC 31 January 1998, the convection moves slightly to the southeast covering west Kalimantan, east Java, and northern Australia. The NRL/NCSU model does not really capture this movement. Instead, it simulates smaller area of rainfall over

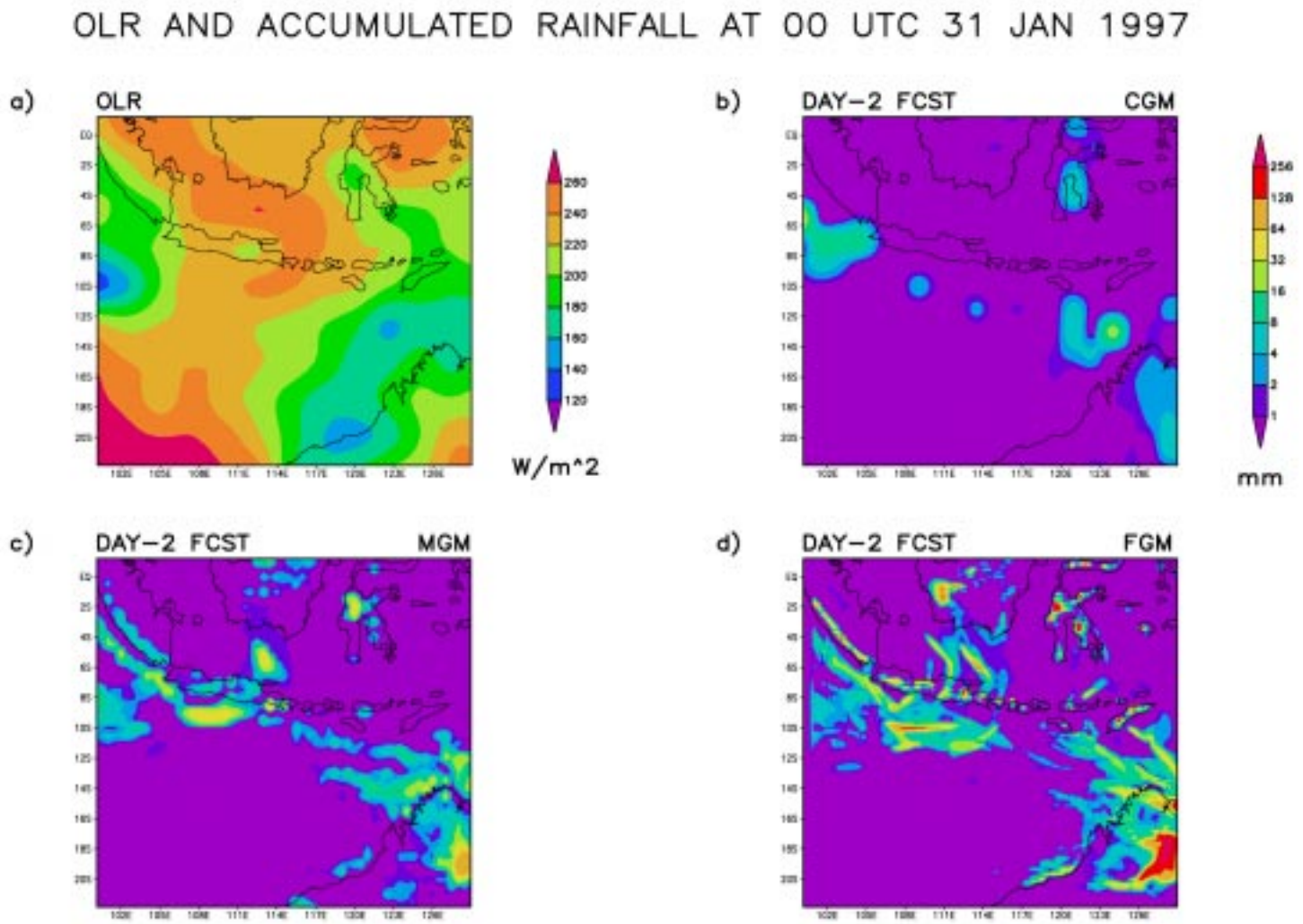

Figure 8.33. a) The OLR distribution and day-2 simulated accumulated rainfall ending at 00 UTC 31 January 1997 in b) CGM, c) MGM, and d) FGM grid resolutions for the Indonesia case from the NRL/NCSU model.

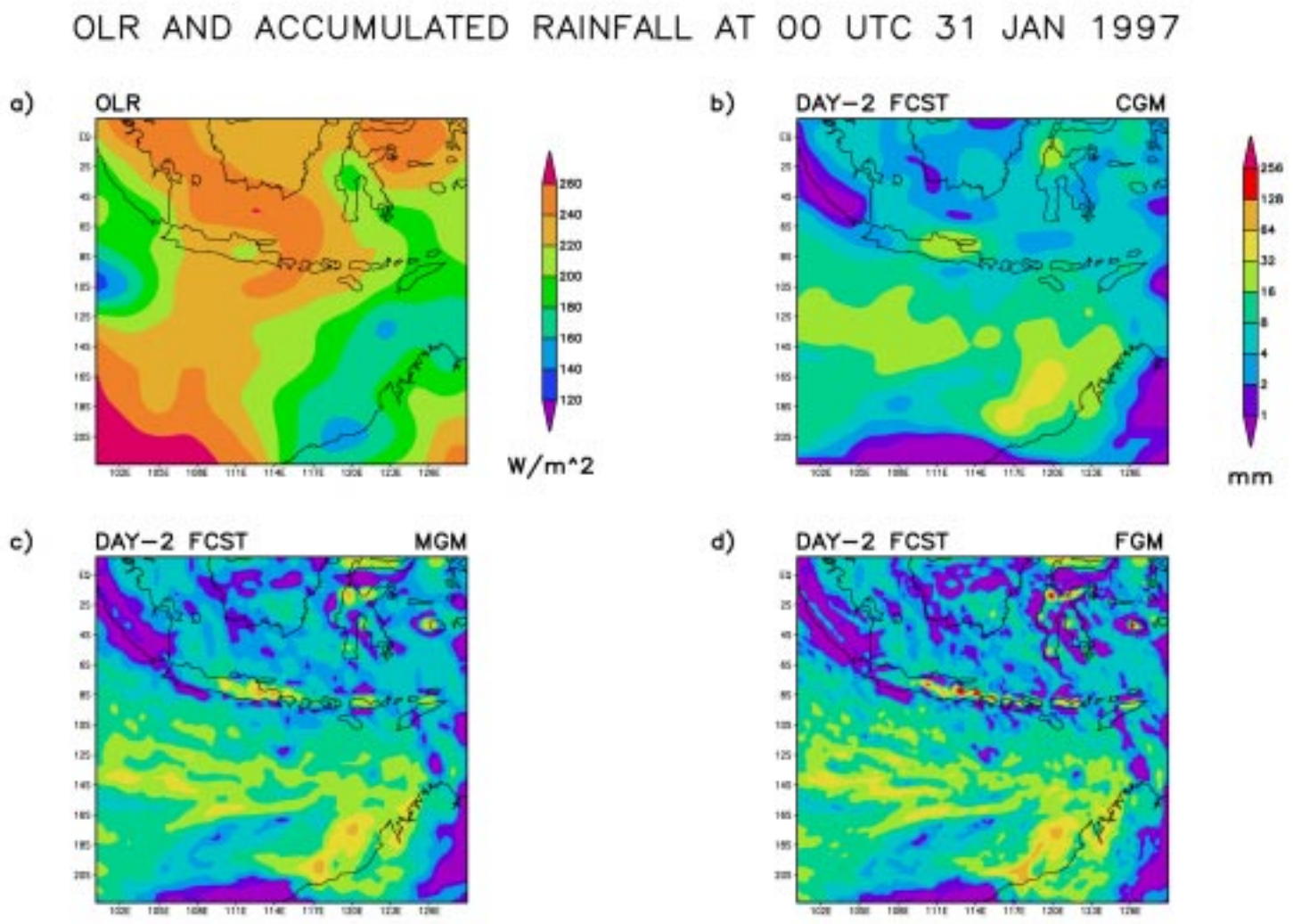

Figure 8.34. As in Fig. 8.33, except from the PSU-NCAR MM5.

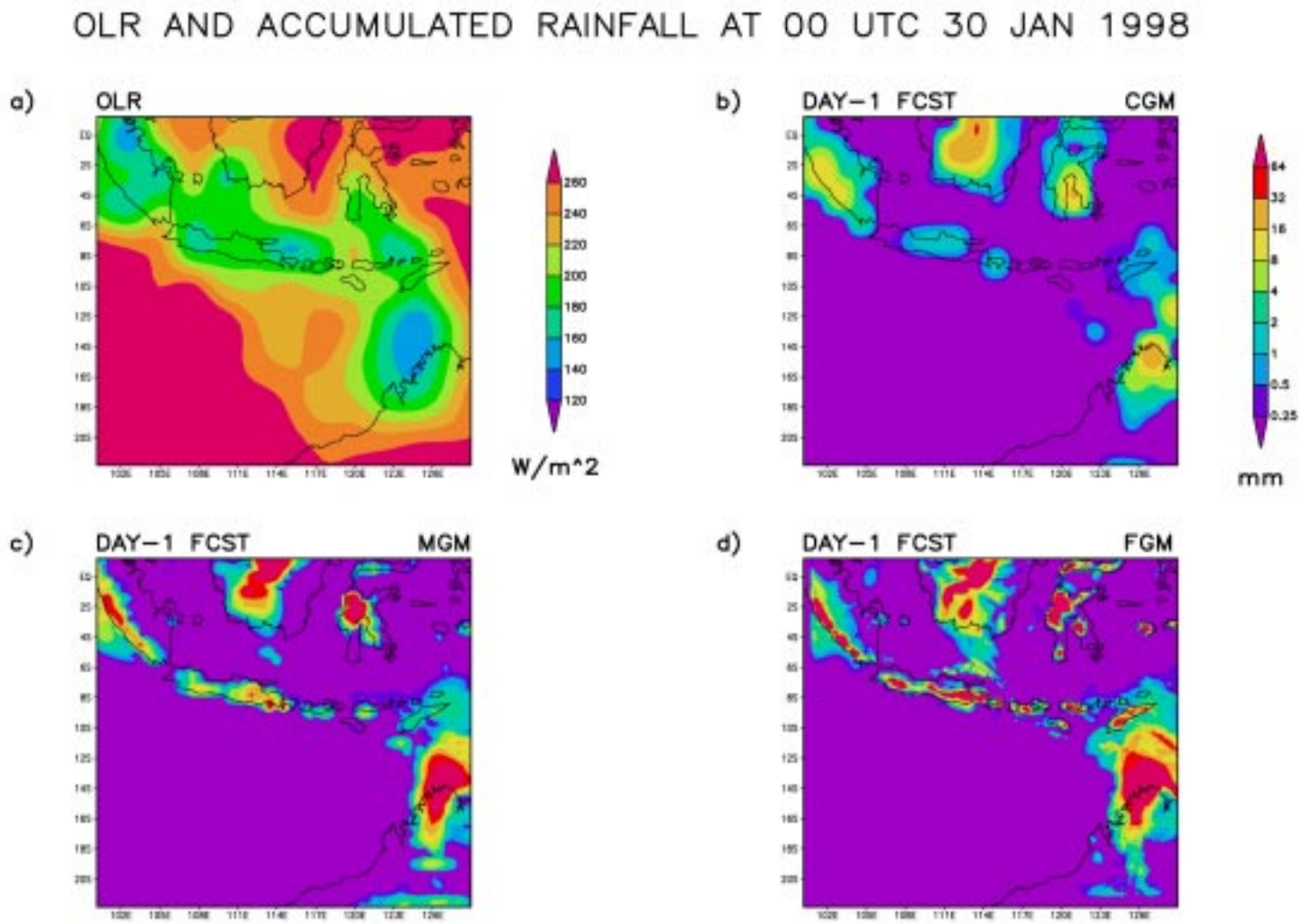

Figure 8.35. a) The OLR distribution and day-1 simulated accumulated rainfall ending at 00 UTC 30 January 1998 in b) CGM, c) MGM, and d) FGM grid resolutions for the Indonesia case from the NRL/NCSU model.

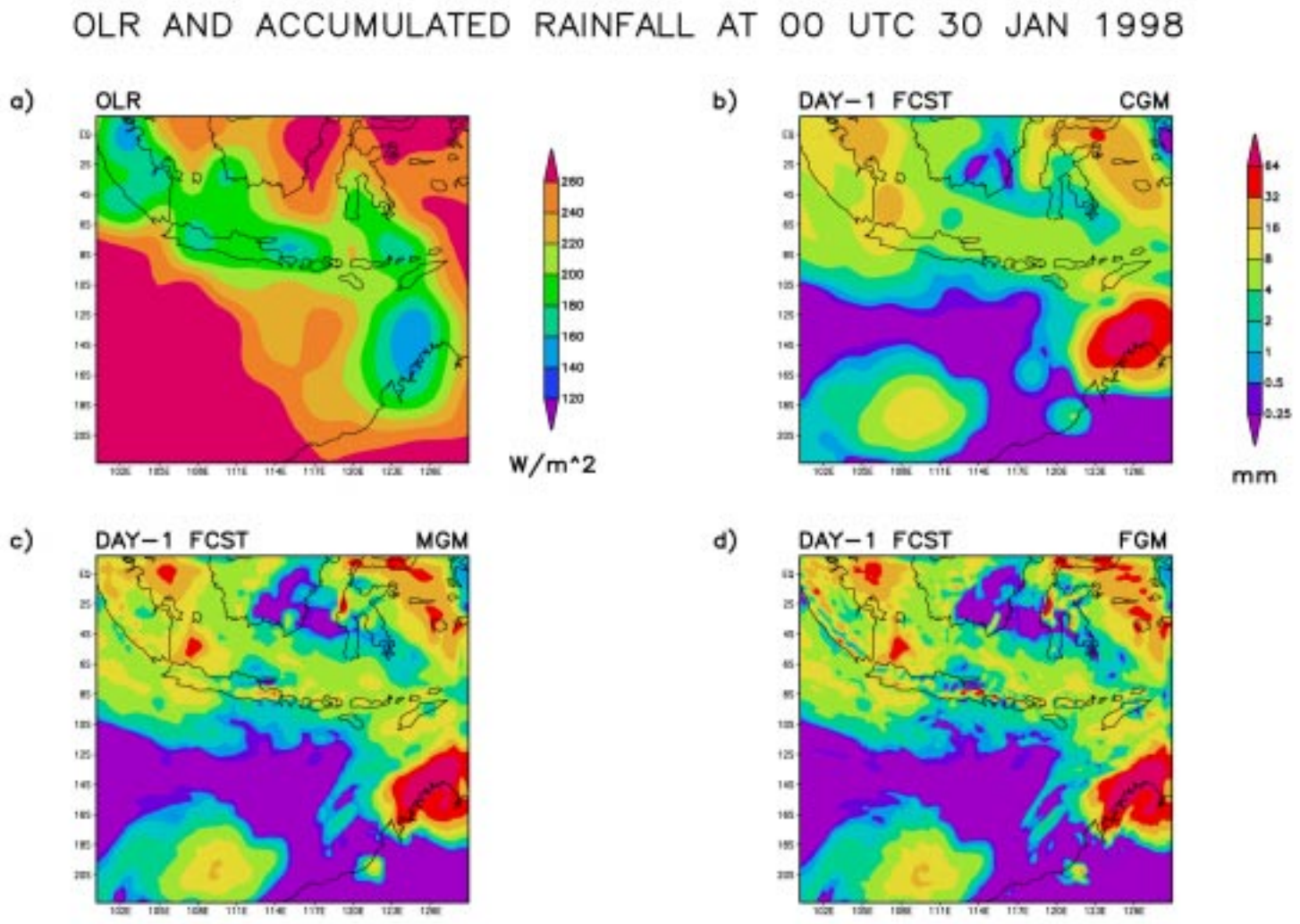

Figure 8.36. As in Fig. 8.35, except from the PSU-NCAR MM5.

the lands than a day before (Figs. 8.37a-d). The PSU-NCAR MM5 still simulates almost the same spatial distribution of rain with lower rain rates (Figs. 8.38a-d).

8.2.3 Zonal Vertical Cross Section of Vertical Velocity, Specific Humidity, and Temperature

Figures 8.39a-c show day-1 simulated mean meridional average vertical velocity, specific humidity and temperature difference for the region between 8°S and 16°S for 00 UTC 30 January 1997. It is clear that the rising motions located over the southeastern Indian Ocean between 106°E and 128°E are associated with strong westerly convergent winds and high SSTs (Fig. 8.39a). The specific humidity profiles, particularly those in the lower troposphere, closely resemble the profiles of profiles of vertical velocity (Fig. 8.39b). The moistened atmosphere is associated with rising motions in the southeastern Indian Ocean. Figure 8.39c displays a rapid increase of temperature with height from surface to about 450 hPa and reverse conditions above it. This warming of the troposphere is probably due to the underlying warm SSTs.

Figures 8.40a-c show day-1 simulated mean meridional vertical velocity, specific humidity and temperature difference for 00 UTC 30 January 1998. The rising motions and the moistening of the atmosphere are mainly found in a small region of the southeastern Indian Ocean, while the sinking motions and the drying of the atmosphere is simulated in the rest of the domain (Figs. 8.40a-b). These profiles do correspond with the convection over northern Australia and suppressed convective activity in the Indonesian-eastern Indian Ocean domain. The temperature profiles reveal that warming of the troposphere is associated with increased SSTs.

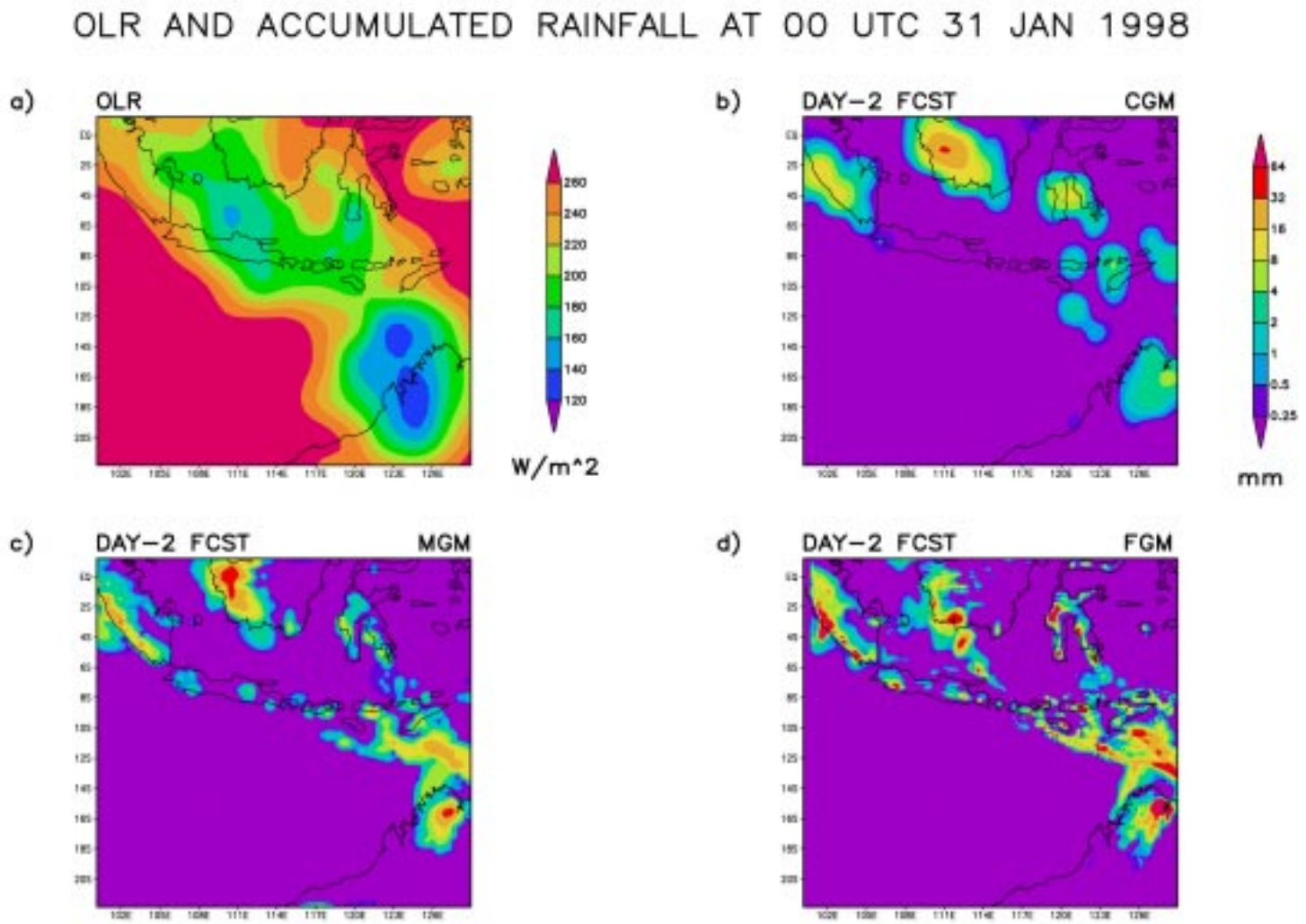

Figure 8.37. a) The OLR distribution and day-2 simulated accumulated rainfall ending at 00 UTC 31 January 1998 in b) CGM, c) MGM, and d) FGM grid resolutions for the Indonesia case from the NRL/NCSU model.

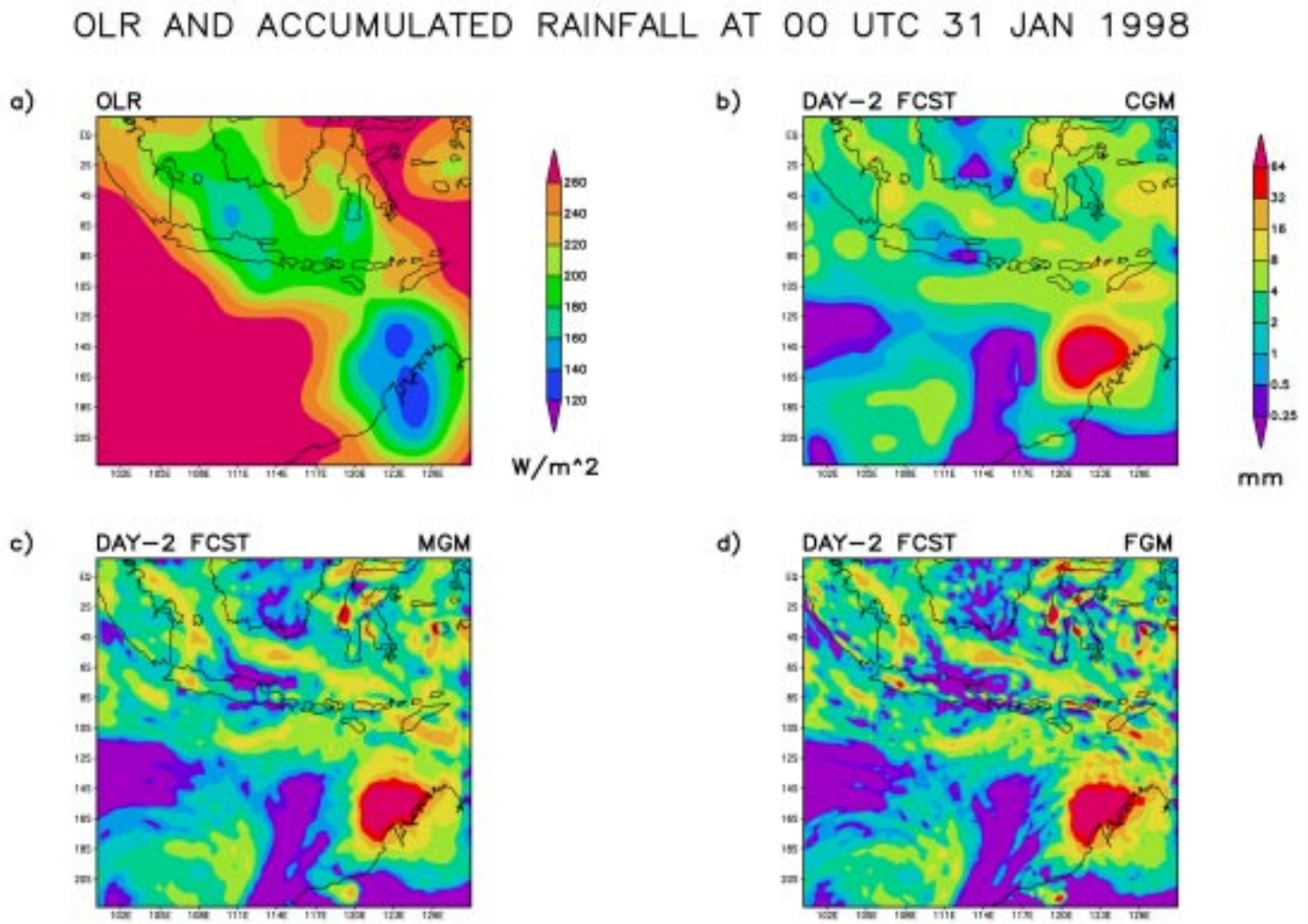

Figure 8.38. As in Fig. 8.37, except from the PSU-NCAR MM5.

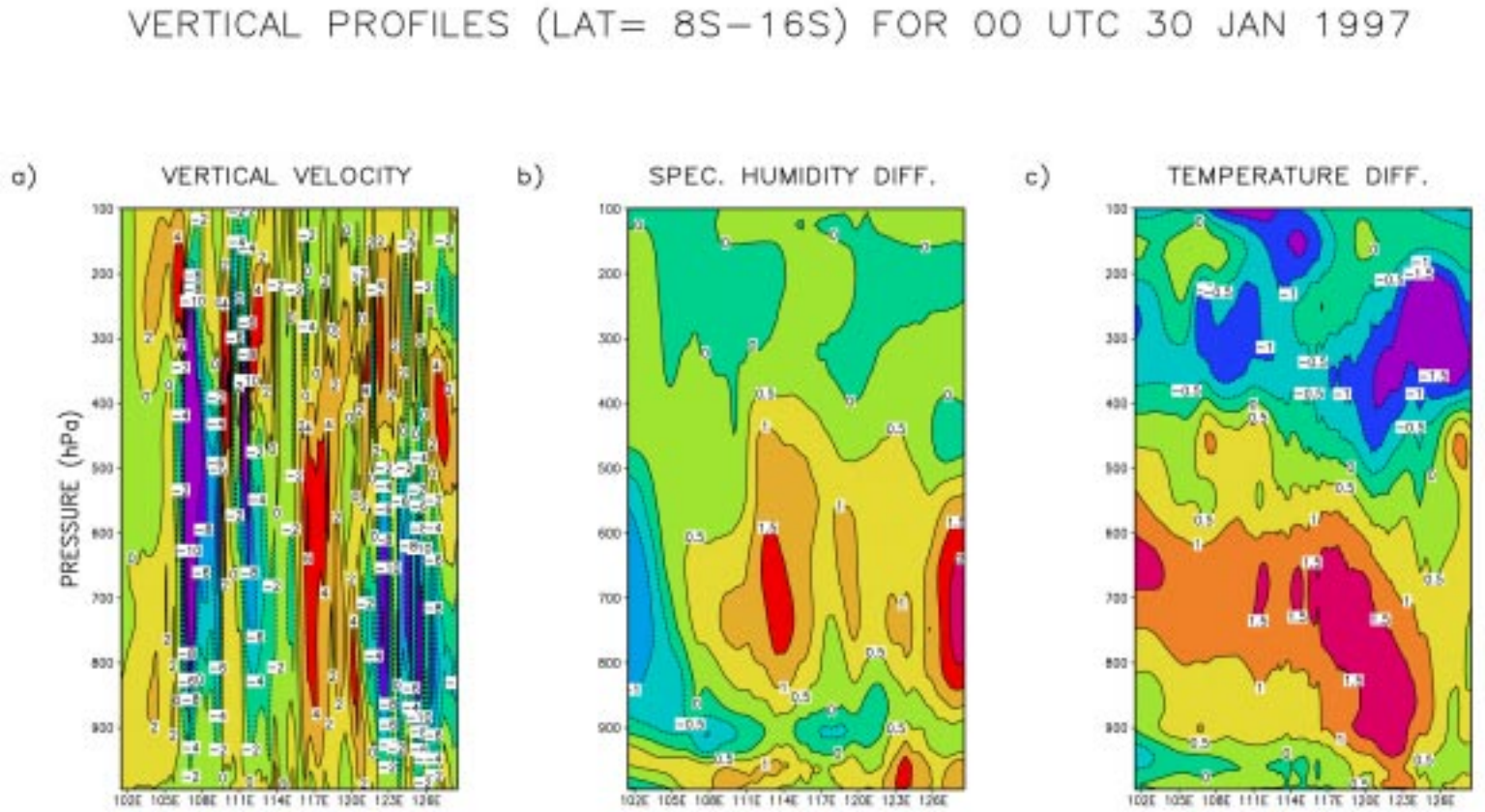

Figure 8.39. Zonal cross sections averaged between 8°S and 16°S of day-1 a) simulated vertical velocity (mb/hr), b) specific humidity (g/kg) and c) temperature (K) differences between model simulation and analysis for 00 UTC 30 January 1997 for the Indonesia case from the NRL/NCSU model.

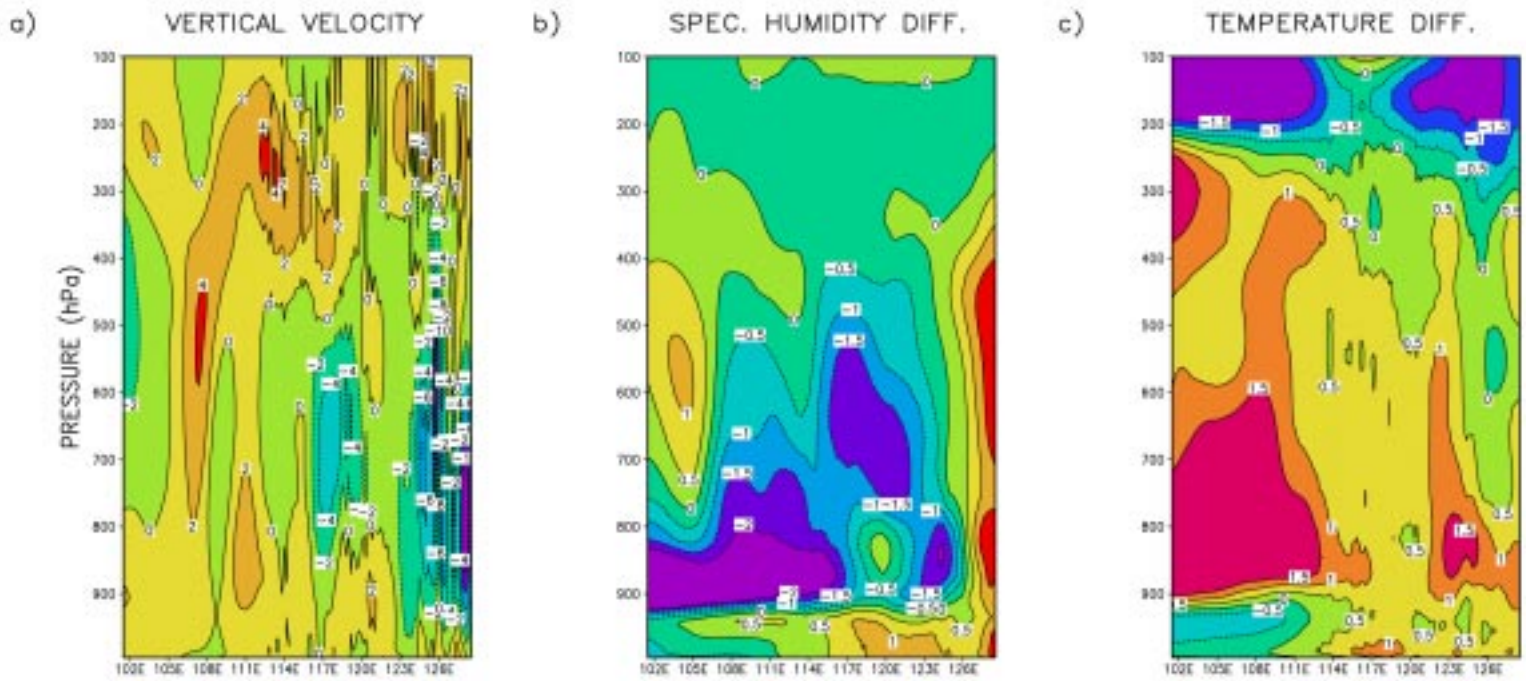

Figure 8.40. As in Fig. 8.39, except for 00 UTC 30 January 1998.

In summary, the ability of the NRL/NCSU model and the PSU-NCAR MM5 to simulate short-range (≤ 2 days) features of the northeast monsoon over the Indian Ocean and Indonesia associated with two contrasting oceanic environments at 00 UTC 29-31 January 1997 and 00 UTC 29-31 January 1998 are studied.

During the 24 hours of integration, the NRL/NCSU model and the PSU-NCAR MM5 are able to simulate most of major features of the monsoon such as mean circulations and oceanic/land mass rainfall reasonably. However, the PSU-NCAR MM5 has difficulty in simulating the distribution of rainfall. During the 48 hours of integration, differences between the models and analyses lower the overall forecast skills. It is found that both models have difficulty to maintain and generate wind flows during the 1997 active monsoon characterized by stronger westerly winds.

Correct treatment of physical processes in the atmosphere boundary condition, the initial conditions, as well as the representation of the orography and surface boundary conditions are of crucial importance for monsoon forecasting. Moreover, accurate simulations of rainfall on day-to-day basis throughout monsoon episode are sensitive to large-scale dynamical and SST forcings.